Organic Letters

Letter

pubs.acs.org/OrgLett

Bis- and Tris-fused Tetrathiafulvalenes Extended with Anthracene-9,10-diylidene

Daisuke Ogi,[†] Yusuke Fujita,[†] Shigeki Mori,[‡,§] Takashi Shirahata,*[,†,§] and Yohji Misaki*[,†,§]

[†]Department of Applied Chemistry, Graduate School of Engineering, Ehime University, 3 Bunkyo-cho, Matsuyama, Ehime 790-8577, Japan

[‡]Advanced Research Support Center, Ehime University, 2-5 Bunkyo-cho, Matsuyama, Ehime 790-8577, Japan

[§]Research Unit for Power Generation and Storage Materials, Ehime University, Matsuyama, Ehime 790-8577, Japan

Supporting Information

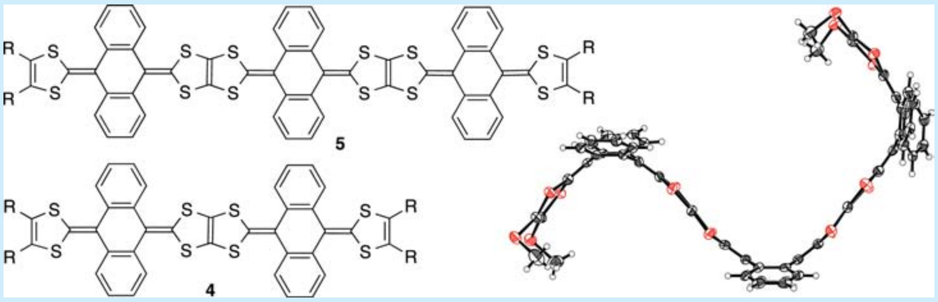

ABSTRACT: Bis- and tris-fused π-electron donors composed of extended tetrathiafulvalene with anthraquinoid spacers (**4** and **5**) were successfully synthesized. X-ray structure analysis of tetrakis(methylthio)-**5** (**5a**) revealed that the molecule adopted a *transoid*−*cisoid* conformation. The cyclic voltammogram of **4a** is composed of two pairs of two-electron redox waves, while the cyclic voltammogram of tetrakis(hexylthio) derivative **5b** consists of one pair of four-electron redox waves and one pair of two-electron redox waves, respectively. Spectroelectrochemistry of **4a** and ^{1}H NMR spectrum of a **4b** salt revealed that two positive charges in $\mathbf{4}^{2+}$ are distributed mainly on one TTFAQ (9,10-bis(1,3-dithiol-2-ylidene)-9,10-dihydroanthracene) moiety.

Tetrathiafulvalene (TTF) and its related compounds have been the subject of considerable interest in the development of organic functional materials because of their multistage redox property with low oxidation potentials.[1] Various TTF derivatives, extended TTF analogues, and TTF oligomers have been continuously synthesized so as to develop molecular materials with higher functionality. Among them, multifused TTF systems[2] have played an important role as potential components for organic functional materials because of their multielectron redox property as well as strong intermolecular interactions in the solids. For example, a number of radical cation salts based on bis-fused TTFs, 2,5-bis(1,3-dithiol-2-ylidene)-1,3,4,6-tetrathiapentalene (BDT-TTP or simply TTP, Figure 1),[3] and its derivatives exhibit metallic conducting behavior down to low temperatures (≤4.2 K).[2,4] On the other hand, a tris-fused TTF, 2,2′-bi[5-(1,3-dithiol-2-ylidene)-1,3,4,6-tetrathiapentanylidene] (BDT-TTPY or simply TTPY, Figure 1)[5] and its derivatives have yielded highly conducting iodine complexes.[2,5] Recently, we reported that TTP and TTPY could be also utilized as positive electrode materials for secondary batteries.[6]

Chemical modification of TTP and TTPY might be a versatile strategy for the development of molecular materials exhibiting high functionality.[2] Insertion of a π-electron spacer is one of the most promising modifications. A vinyl analogue of TTP, 2-(1,3-dithiol-2-ylidene)-5-(2-ethanediylidene-1,3-dithiole)-1,3,4,6-tetrathiapentalene (DTEDT, Figure 1), which is designed by insertion of two sp^2 carbon atoms into TTP, has actually afforded an organic superconductor, $(\mathrm{DTEDT})_3\mathrm{Au(CN)}_2$, as well as many molecular conductors retaining metallic conductivity down to ≤4.2 K.[7] On the other hand, rechargeable batteries incorporating tris- and pentakis-fused TTF derivatives inserted with cyclohexene-1,4-diylidenes (TTM-2-CH-3mer and TTM-2,4-CH-5mer, respectively, see also Figure 1) as a positive

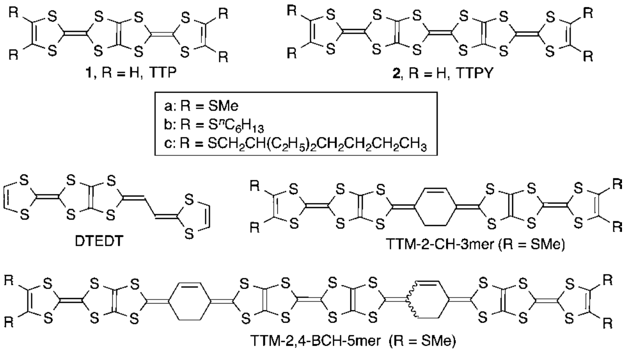

Figure 1. Structures of fused TTF donors.

Received: September 29, 2016
Published: November 4, 2016

DOI: 10.1021/acs.orglett.6b02944
Org. Lett. 2016, 18, 5868−5871

electrode material exhibit high discharge energy density (600–700 mWh g^{-1}) and relatively good cycle performance (72–88% of the first discharge capacity after 20–30 cycles).[8] In this context, development of new multifused π-electron donors containing extended TTF moieties are of interest to explore novel organic functional materials.

An extended TTF with an anthraquinoid spacer and its derivatives (**3**, Figure 2; herein abbreviated "TTFAQ")[9] have received significant attention as building blocks for molecular organic materials such as sensitizers for organic solar cells,[10] ion sensors,[11] molecular receptors,[12] and so on. TTFAQ is known to exhibit a single two-electron oxidation process because the dicationic state is more stable than the radical cationic state.[13] In this connection, fused π-electron donors composed of TTFAQ units are of particular interest as multistage redox systems as well as components for functional materials. We report herein the synthesis, structures, and electrochemical properties of bis- and tris-fused TTFAQ donors **4a**,**b** and **5a**,**b**.[14]

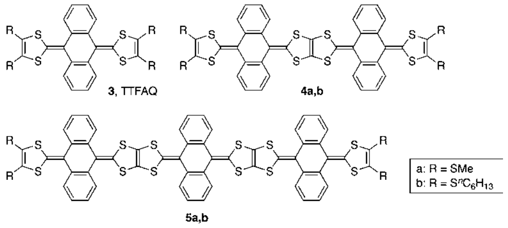

Figure 2. Structures of TTFAQ derivatives **4** and **5**.

New fused donors **4** and **5** were successfully synthesized according to Scheme 1. The triethyl phosphite mediated cross-coupling reaction between **6a**,**b**[15] and 1,3-dithiole-2-thione with a phosphonate moiety (**7**)[16] in chlorobenzene at 140 °C afforded the corresponding TTFAQ derivatives **8a**,**b** in 23 and 26% yields, respectively. The Horner–Wadsworth–Emmons reaction of **8a** with **6a**,**b**, respectively, in the presence of lithium diisopropylamide (LDA) in THF at −78 °C gave the bis-fused donors **4a**,**b** in 53 and 35% yields, respectively. On the other hand, the tris-fused donors **5a**,**b** were obtained in 45 and 35% yields, respectively, by the Horner–Wadsworth–Emmons reaction of anthraquinone (**9**) with 2.2 molar equiv of **8a**,**b** in the presence of LDA in THF at −78 °C. All of the donors were obtained as stable yellow powders.

Scheme 1. Synthesis of 4a,b and 5a,b

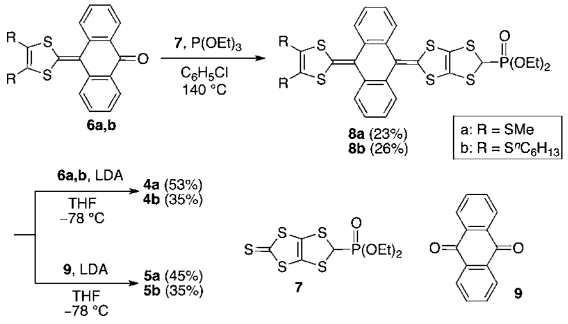

Single crystals of **5a** were grown by slow evaporation of the solvents from a mixed solution of carbon disulfide/*n*-hexane, and platelike crystals with composition of (**5a**)(*n*-hexane)$_{0.5}$ were obtained. The crystal belongs to the triclinic system with a space group of $P\bar{1}$.[17,18] Figure 3 shows the molecular structures of **5a** in (**5a**)(*n*-hexane)$_{0.5}$. The anthraquinoid moieties adopt a saddle-like conformation because of the steric repulsion between the sulfur atoms in 1,3-dithiole rings and the *peri*-hydrogen atoms as observed in most TTFAQ derivatives.[19] The anthraquinoid moieties C6–C7–C12–C19–C18–C13, C24–C25–C30–C37–C36–C31, and C42–C43–C48–C55–C54–C49 adopt a boat conformation with folding angles of 32.9(2)° for the C7–C13 axis, 32.7(2)° for the C12–C18 axis, 31.1(2)° for the C25–C31 axis, 31.7(2)° for the C30–C36 axis, 29.4(2)° for the C43–C49 axis, and 30.3(2)° for the C48–C54 axis. The dihedral angles ϕ_1, ϕ_2, and ϕ_3 between the benzene rings are 139.5(1), 142.0(2), and 142.0(1)°, respectively. The dihedral angles θ_1, θ_2, and θ_3 between the 1,3-dithiole rings are 78.5(2), 77.2(2), and 83.6(2)°, respectively. These angles mentioned above are similar to the precedent.[19]

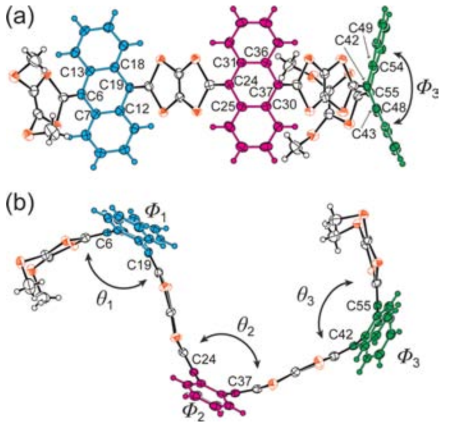

Figure 3. (a) Top view and (b) side view of ORTEP drawings of **5a** in (**5a**)(*n*-hexane)$_{0.5}$. Ellipsoids displayed at 50% probability. The solvent molecule (*n*-hexane) is omitted for clarity.

Compounds **4** and **5** possess multiple anthraquinoid moieties; therefore, there are two and three conformational isomers with respect to the conformations of the anthraquinoid moieties, namely, *transoid* and *cisoid* isomers for **4** and *transoid*–*transoid*, *transoid*–*cisoid*, and *cisoid*–*cisoid* combinations for **5**. Variable-temperature (VT) NMR spectra of **4a** and **5a** were obtained in $Cl_2CDCDCl_2$ over the temperature range from 25 to 100 °C (Figure 4).

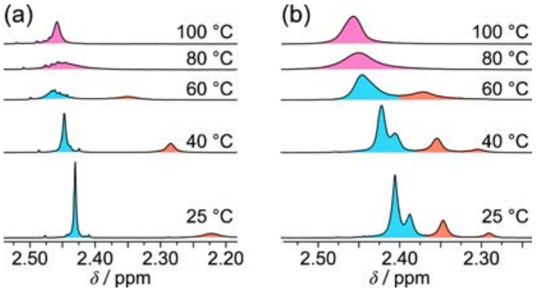

Figure 4. Variable-temperature ^{1}H NMR spectra ($Cl_2CDCDCl_2$, 500 MHz) of (a) **4a** and (b) **5a**.

Multiple peaks for the methyl groups of methylsufanyl (SCH_3) substituents of **4a** and **5a** were observed at room temperature (25 °C), and the coalescence of the isomer peaks is clearly observed at 100 °C. This result indicates that the isomers of **4a** and **5a** exist in solution at room temperature. The crystallization of the *transoid*–*cisoid* isomer of **5a** is not attributed to its stability

DOI: 10.1021/acs.orglett.6b02944
Org. Lett. 2016, 18, 5868–5871

compared with those of the other isomers, where the *transoid*−*transoid* isomer is calculated to be more stable than the *transoid*−*cisoid* isomer by 0.25 kcal mol^{-1} from the density functional theory (DFT) calculation (Figure S2)[20] but is associated with the lattice energy and the intermolecular interactions (Figure S1).

Electrochemical properties of **4a** and **5b** were investigated by cyclic voltammetry. Figure 5 shows deconvoluted cyclic voltammograms of **4a** and **5b** measured in a benzonitrile−carbon disulfide solution (1:1, v/v). Both donors exhibit two pairs of redox waves. Peak currents of the both anodic waves of **4a** are comparable to each other. Considering that **4a** has four redox-active 1,3-dithiol-2-ylidene (DT) units, both oxidation waves of **4a** might correspond to the two-electron transfer process. On the other hand, the peak current of the first oxidation wave of **5b** is about twice as large as that of the second oxidation wave. This result indicates the first oxidation wave of **5b** corresponds to the four-electron transfer process and the other to the two-electron transfer process because of the presence of six DT units in **5b**.

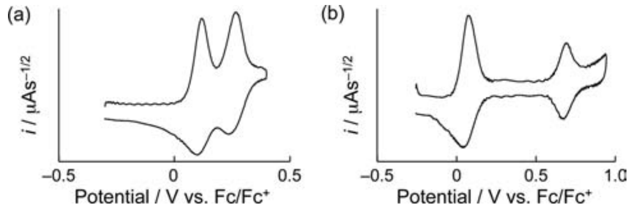

Figure 5. (a) Deconvoluted cyclic voltammograms of **4a** and (b) **5b** in a benzonitrile−carbon disulfide solution (1:1, v/v) containing $^nBu_4N{\cdot}PF_6$ (0.1 M) at 25 °C. Experimental conditions: Pt working and counter electrodes, scan rate 0.005 V s^{-1}. Potentials were measured against Ag/Ag^+ electrode and converted to the value vs Fc/Fc^+.

The redox potentials of **4a** and **5b** are summarized in Table 1 together with their related compounds. The first redox potentials of **4a** (E_{m1} = +0.10 V vs Fc/Fc^+) and **5b** (E_M = +0.06 V) are comparable to the redox potentials of **3a** (E_{m1} = +0.07 V). In contrast, the potential corresponding to the $\mathbf{5b}^{6+}$/**5b** redox couple (E_{m3} = +0.68 V) is significantly more positive by 0.43 V than that of the $\mathbf{4a}^{4+}$/**4a** redox (E_{m2} = +0.25 V). Such a considerable positive shift of the maximum redox potentials suggests that $\mathbf{5b}^{6+}$ is more destabilized than $\mathbf{4a}^{4+}$ because of large on-site Coulomb repulsion among six positive charges in $\mathbf{5b}^{6+}$. The E_{m1} of **4a** and E_M of **5b** are comparable to those of the corresponding fused TTF derivatives **1a**[21] (E_1 = +0.11 V) and **2c**[22] (E_1 = +0.12 V), respectively. On the other hand, the potentials corresponding to maximum electrons redox of **4a** (E_{m2}) and **5b** (E_{m3}) are lower by 0.42 and 0.19 V than those of **1a** (E_4 = +0.67 V) and **2c** (E_{m3} = +0.87 V), respectively. The negative shifts of the potentials corresponding to maximum electrons redox in **4a** and **5b** might be attributed to reducing on-site Coulomb repulsion between positive charges by insertion of orthogonally arranged anthracene spacers in $\mathbf{4a}^{4+}$ and $\mathbf{5b}^{6+}$.

Table 1. Redox Potentials[a] of 4a, 5b, and Related Compounds

	E_1	E_2	E_3	E_4	E_5	E_6
	E_{m1}[b]	E_M[b]	E_{m2}[b]		E_{m3}[b]	
4a	+0.10 (2e)		+0.25 (2e)			
5b		+0.06 (4e)			+0.68 (2e)	
3a	+0.07 (2e)					
1a	+0.11	+0.28	+0.54	+0.67		
2c	+0.12	+0.19	+0.39 (2e)		+0.87 (2e)	

[a] V vs Fc/Fc^+. [b] $E_{m1} = (E_1 + E_2)/2$. $E_{m2} = (E_3 + E_4)/2$. $E_{m3} = (E_5 + E_6)/2$. $E_M = (E_1 + E_2 + E_3 + E_4)/4$.

Spectroelectrochemistry of **4a** and **5b** was investigated to elucidate the electronic structures of their oxidative species. Figure 6a shows the UV−vis−NIR spectra of **4a** and its oxidative species generated by applying constant voltages in a benzonitrile solution. When the voltage at +0.11 V (vs Fc/Fc^+) was applied, new absorption bands presumably attributed to $\mathbf{4a}^{2+}$ appeared at 360, 382, 427, and 606 nm, respectively. Further application of constant voltages at +0.41 V gave a spectrum probably ascribed to $\mathbf{4a}^{4+}$ at 384, 401, 426, 474, and 585 nm, respectively. The spectra of $\mathbf{4a}^{2+}$ and $\mathbf{4a}^{4+}$ have a resemblance to that of $\mathbf{3a}^{2+}$ (382, 394, 421, and 486 nm) except for the shoulder band at around 600 nm.[12] These results suggest that two positive charges in $\mathbf{4a}^{2+}$ are distributed mainly over one of the TTFAQ units as shown in Figure 7. As for **5c**, the spectra probably derived from $\mathbf{5c}^{4+}$ and $\mathbf{5c}^{6+}$ were obtained by applying voltages of +0.26 and +0.91 V, respectively (Figure 6b), and both spectra considerably resemble each other. The shapes of those spectra are also close to those of $\mathbf{4a}^{2+}$ and $\mathbf{3a}^{2+}$, suggesting that each two positive charges might be located mainly on the two TTFAQ units in $\mathbf{5b}^{4+}$. In addition to this, observation of a simultaneous four-electron transfer wave in cyclic voltammetry indicates that two $TTFAQ^{2+}$ units are located at the both ends (see also Figure 7). In that case, significant reduction of on-site Coulomb repulsion in $\mathbf{5b}^{4+}$ is expected due to presence of the electron-rich TTFAQ spacer between two dicationic TTFAQ units.

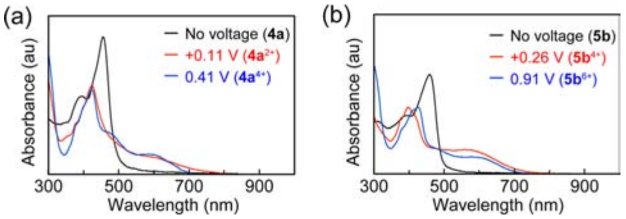

Figure 6. UV−vis−NIR spectra of (a) **4a**, (b) **5b**, and their oxidative species generated by applying a constant voltage in a benzonitrile solution.

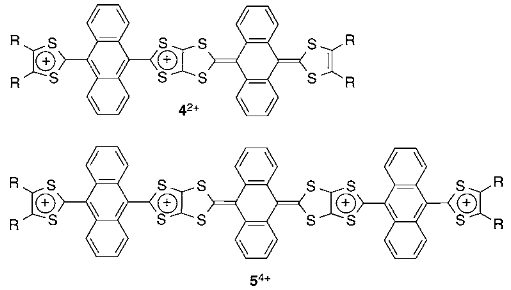

Figure 7. Plausible structures of 4^{2+} and 5^{4+}.

Isolation of $\mathbf{4b}^{2+}$ and $\mathbf{5a}^{4+}$ salts was carried out by chemical oxidation of **4b** or **5a** with $(p\text{-}BrC_6H_4)_3N^{\bullet+}SbCl_6^-$ in CH_2Cl_2−CH_3CN at room temperature. The ^1H NMR spectrum of the $\mathbf{5a}^{4+}$ salt in DMSO-d_6 exhibited a signal assigned to the SCH_3 protons at 3.00 ppm (Figure S20). The chemical shift of the SCH_3 protons was same as that of $\mathbf{3a}^{2+}$ (3.00 ppm), indicating that $\mathbf{5}^{4+}$ has a structure with two $(TTFAQ)^{2+}$ units at both ends as shown in Figure 7. As for the ^{1}H NMR spectrum of the **4b**$^{2+}$ salt in CD_3CN, two signals corresponding to SCH_2 protons were observed at 2.87 and 3.42 ppm, where the proton integral ratio of two parts of SCH_2 was almost 1:1 Figure S19). The chemical shifts of both signals were close to those of the SCH_2 protons of **5b** (2.81 ppm) and **5b**$^{4+}$ (3.42 ppm) (Figure S21). Those results strongly support the proposed structure of **4**$^{2+}$ as shown in Figure 7.[23]

In summary, we have developed new bis- and tris-fused π-electron donors composed of TTAQ units (**4** and **5**). Both donors exhibited a simultaneous two- or four-electron oxidation process because of the presence of the TTFAQ moieties. The positive charges in **4a**$^{2+}$ and **5b**$^{4+}$ are not delocalized over the whole molecules but are located on a part of the TTFAQ units. Large positive shifts of the maximum-electron redox potentials by fusion of the TTFAQ units suggest that new donors **4** and **5** are applicable to positive electrode materials for rechargeable batteries with high energy densities. Further investigations including synthesis of tetrakis- and pentakis-fused analogues as well as the charge−discharge performance of rechargeable batteries incorporating **4** and **5** as positive electrode materials are actively in progress.

ASSOCIATED CONTENT

Supporting Information

The Supporting Information is available free of charge on the ACS Publications website at DOI: 10.1021/acs.orglett.6b02944.

> Detailed experimental procedures and NMR spectra of all new compounds; crystal structure of (**5a**)(n-hexane)$_{0.5}$; optimized structures of **4a**, the HOMO and HOMO-n of **4a** (n = 1), and **5a** (n = 1, 2); UV−vis−NIR spectra of **4a**$^{2+}$ and **5a**$^{4+}$ (PDF)
>
> X-ray data for (**5a**)(n-hexane)$_{0.5}$ (CIF)

AUTHOR INFORMATION

Corresponding Authors

*E-mail: shirahata.takashi.mj@ehime-u.ac.jp.
*E-mail: misaki.yohji.mx@ehime-u.ac.jp.

Notes

The authors declare no competing financial interest.

ACKNOWLEDGMENTS

This work was partially supported by JSPS KAKENHI Grant Nos. JP23550155, JP26410095, and JP15H00948, by MEXT KAKENHI Grant No. JP15H03798, and by Grant-in-Aid for Research Promotion, Ehime University, to The Research Unit for Power Generation and Storage Materials.

REFERENCES

(1) (a) Canevet, D.; Sallé, M.; Zhang, G.; Zhang, D.; Zhu, D. *Chem. Commun.* **2009**, 2245. (b) *TTF Chemistry—Fundamental and Applications of Tetrathiafulvalene*; Yamada, J., Sugimoto, T., Eds.; Kodansha-Springer: Tokyo, 2004. (c) Gorgues, A.; Hudhomme, P.; Sallé, M. *Chem. Rev.* **2004**, *104*, 5151. (d) Segura, J. L.; Martín, N. *Angew. Chem., Int. Ed.* **2001**, *40*, 1372. (e) Iyoda, M.; Hasegawa, M.; Miyake, Y. *Chem. Rev.* **2004**, *104*, 5085. (f) Hasegawa, M.; Iyoda, M. In *Organic Redox Systems*; Nishinaga, T., Ed.; Wiley, 2016; pp 89.

(2) Misaki, Y. *Sci. Technol. Adv. Mater.* **2009**, *10*, 024301.

(3) Misaki, Y.; Matsui, T.; Kawakami, K.; Nishikawa, H.; Yamabe, T.; Shiro, M. *Chem. Lett.* **1993**, *22*, 1337.

(4) Misaki, Y.; Fujiwara, H.; Yamabe, T.; Mori, T.; Mori, H.; Tanaka, S. *Chem. Lett.* **1994**, *23*, 1653.

(5) (a) Nishikawa, H.; Kawauchi, S.; Misaki, Y.; Yamabe, T. *Chem. Lett.* **1996**, *25*, 43. (b) Misaki, Y.; Kawakami, K.; Higuchi, N.; Nishikawa, H.; Yamabe, T. *Mol. Cryst. Liq. Cryst. Sci. Technol., Sect. A* **1996**, *284*, 337.

(6) Inatomi, Y.; Hojo, N.; Yamamoto, T.; Watanabe, S.; Misaki, Y. *ChemPlusChem* **2012**, *77*, 973.

(7) Misaki, Y.; Higuchi, N.; Fujiwara, H.; Yamabe, T.; Mori, T.; Mori, H.; Tanaka, S. *Angew. Chem., Int. Ed. Engl.* **1995**, *34*, 1222.

(8) (a) Kato, M.; Ogi, D.; Yao, M.; Misaki, Y. *Chem. Lett.* **2013**, *42*, 1556. (b) Kato, M.; Senoo, K.; Yao, M.; Misaki, Y. *J. Mater. Chem. A* **2014**, *2*, 6747.

(9) (a) Akiba, K.; Ishikawa, K.; Inamoto, N. *Bull. Chem. Soc. Jpn.* **1978**, *51*, 2674. (b) Bryce, M. R.; Moore, A. J. *Synth. Met.* **1988**, *25*, 203. (c) Bryce, M. R.; Moore, A. J.; Hasan, M.; Ashwell, G. J.; Fraser, A. T.; Clegg, W.; Hursthouse, M. B.; Karaulov, A. I. *Angew. Chem., Int. Ed. Engl.* **1990**, *29*, 1450.

(10) (a) Martín, N.; Sánchez, L.; Herranz, M. Á.; Illescas, B.; Guldi, D. M. *Acc. Chem. Res.* **2007**, *40*, 1015. (b) Wenger, S.; Bouit, P.-A.; Chen, Q.; Teuscher, J.; Censo, D. D.; Humphry-Baker, R.; Moser, J.-E.; Delgado, J. L.; Martín, N.; Zakeeruddin, S. M.; Grätzel, M. *J. Am. Chem. Soc.* **2010**, *132*, 5164.

(11) Hardouin-Lerouge, M.; Chesneau, B.; Allain, M.; Hudhomme, P. *J. Org. Chem.* **2012**, *77*, 2441.

(12) (a) Isla, H.; Gallego, M.; Pérez, E. M.; Viruela, R.; Ortí, E.; Martín, N. *J. Am. Chem. Soc.* **2010**, *132*, 1772. (b) Bivaud, S.; Goeb, S.; Croué, V.; Dron, P. I.; Allain, M.; Salle, M. *J. Am. Chem. Soc.* **2013**, *135*, 10018.

(13) (a) Gruhn, N. E.; Macías-Ruvalcaba, N. A.; Evans, D. H. *Langmuir* **2006**, *22*, 10683. (b) Jones, A. E.; Christensen, C. A.; Perepichka, D. F.; Batsanov, A. S.; Beeby, A.; Low, P. J.; Bryce, M. R.; Parker, A. W. *Chem. - Eur. J.* **2001**, *7*, 973.

(14) Synthesis of dimeric and trimeric TTFAQ derivatives linked by a spacer was reported. For examples, see: (a) Martín, N.; Pérez, I.; Sánchez, L.; Seoane, C. *J. Org. Chem.* **1997**, *62*, 870. (b) Christensen, C. A.; Bryce, M. R.; Batsanov, A. S.; Becher, J. *Org. Biomol. Chem.* **2003**, *1*, 511. (c) Huerta, E.; Isla, H.; Pérez, E. M.; Bo, C.; Martín, N.; Mendoza, J. *J. Am. Chem. Soc.* **2010**, *132*, 5351.

(15) (a) Bryce, M. R.; Finn, T.; Moore, A. J.; Batsanov, A. S.; Howard, J. A. K. *Eur. J. Org. Chem.* **2000**, *2000*, 51. (b) Christensen, C. A.; Batsanov, A. S.; Bryce, M. R. *J. Org. Chem.* **2007**, *72*, 1301.

(16) Misaki, Y.; Nishikawa, H.; Kawakami, K.; Uehara, T.; Yamabe, T. *Tetrahedron Lett.* **1992**, *33*, 4321.

(17) Crystallographic data reported in this manuscript have been deposited with the Cambridge Crystallographic Data Centre as supplementary publication no. CCDC-1510578. Copies of the data can be obtained free of charge via http://www.ccdc.cam.ac.uk/conts/retrieving.html (or from the Cambridge Crystallographic Data Centre, 12, Union Road, Cambridge, CB2 1EZ, U.K.; fax: + 44 1223 336033; or deposit@ccdc.cam.ac.uk).

(18) Crystal data of (**5a**)(n-hexane)$_{0.5}$: triclinic, $P\bar{1}$ (#2), a = 12.310(4) Å, b = 14.356(6) Å, c = 18.752(8) Å, α = 82.396(12)°, β = 76.856(13)°, γ = 70.392(12)°, V = 3034(2) Å^3, $R1$ = 0.0848, $wR2$ = 0.1867 for observed 10150 reflections ($I > 2\sigma(I)$), GOF = 1.134.

(19) (a) Christensen, C. A.; Bryce, M. R.; Batsanov, A. S.; Howard, J. A. K.; Jeppesen, J. O.; Becher, J. *Chem. Commun.* **1999**, 2433. (b) Bivaud, S.; Goeb, S.; Croué, V.; Dron, P. I.; Allain, M.; Sallé, M. *J. Am. Chem. Soc.* **2013**, *135*, 10018. (c) Christensen, C. A.; Bryce, M. R.; Batsanov, A. S.; Becher, J. *Org. Biomol. Chem.* **2003**, *1*, 511.

(20) All of the DFT calculations were performed with the Gaussian09 program package. See the Supporting Information for more details.

(21) Misaki, Y.; Nishikawa, H.; Kawakami, K.; Koyanagi, S.; Yamabe, T.; Shiro, M. *Chem. Lett.* **1992**, *21*, 2321.

(22) Compound **2c** was newly prepared according to ref 5.